

High-Resolution DOA Estimation via a Novel Tree Model-based Deep Neural Network

Yifan Li, Feng Shu, *Member, IEEE*, Jun Zou, Wei Gao, Yaoliang Song, and Jiangzhou Wang, *Fellow, IEEE*

Abstract—To satisfy the high-resolution requirements of direction-of-arrival (DOA) estimation, conventional deep neural network (DNN)-based methods using grid idea need to significantly increase the number of output classifications and also produce a huge high model complexity. To address this problem, a multi-level tree-based DNN model (TDNN) is proposed as an alternative, where each level takes small-scale multi-layer neural networks (MLNNs) as nodes to divide the target angular interval into multiple sub-intervals, and each output class is associated to a MLNN at the next level. Then the number of MLNNs is gradually increasing from the first level to the last level, and so increasing the depth of tree will dramatically raise the number of output classes to improve the estimation accuracy. More importantly, this network is extended to make a multi-emitter DOA estimation. Simulation results show that the proposed TDNN performs much better than conventional DNN and root-MUSIC at extremely low signal-to-noise ratio (SNR), and can achieve Cramer-Rao lower bound (CRLB). Additionally, in the multi-emitter scenario, the proposed Q -TDNN has also made a substantial performance enhancement over DNN and Root-MUSIC, and this gain grows as the number of emitters increases.

Index Terms—direction-of-arrival (DOA) estimation, deep neural network (DNN), multi-sources, multi-label learning.

I. INTRODUCTION

Direction-of-arrival (DOA) estimation has been a widely studied topic in wireless communications, array signal processing, radar and sonar for few decades [1]. One of the most important directions is how to improve the estimation precision, especially in poor signal conditions such as low signal to noise ratio (SNR) and low number of snapshots. In recent years, with the development of massive MIMO technology, some works considered massive receive arrays for improving the spatial resolution and DOA estimation precision [2] [3].

Nowadays, deep learning (DL) techniques have been introduced into DOA estimation, by matching the principles of DOA estimation with the frameworks of supervised learning. Many high-precision methods can be trained via prior DOA data for various scenarios. [4] proposed a deep neural network (DNN) structure for super-resolution channel estimation and DOA estimation based on massive MIMO system. A DNN-based method was also proposed for hybrid massive MIMO systems with uniform circular arrays (UCA) in [5]. Convolutional neural network (CNN) is another technique widely

considered in DOA estimation, like [6] designed a CNN-based method for improving precision in low SNR, and [7] introduced CNN for DOA estimation with sparse prior. Overall, traditional DL-based DOA estimation methods usually employ a flat single-level network structure, each output class corresponding to a specific direction and the estimation results can only be generated from these fixed directions. So they have high-resolution for on-grid DOAs and have accuracy lower bounds much higher than Cramer-Rao lower bound (CRLB) for off-grid DOAs [8]. Then conventional single-network models have to increase the number of output classes to improve spatial resolution and also cause the serious increase of model complexity.

In addition, how to apply the multi-label learning algorithms for the multi-emitter cases is also a key problem in DOA estimation with DL techniques. Traditional multi-label learning algorithms like binary relevance, label ranking, multi-class classification can transform complex multi-labeling problems into more accessible single-labeling problems, and methods with another idea are working to apply existing machine learning algorithms to multi-label learning, such as multi label ML-kNN, ML-DT, ML-SVM, etc. [9]. Then based on the ideas of multi-labeling learning, [10] applied the DNN model for DOA estimation of multi targets, but the DOA estimation accuracy will significantly decrease with the growth of source number and method to improve the resolution of multi-emitter DOA estimation will be studied in this work.

In order to address the problems of DL-based DOA estimation, a novel DNN architecture called TDNN is studied in this work and a high-resolution TDNN-based multi-emitter estimator is also proposed. Then the main contributions of this work are summarized as follows:

- 1) To improve the DOA estimation accuracy and decrease the model complexity of single network, a multi-level tree-based DNN model is proposed, where each level uses small-scale MLNNs as nodes to divide the angular interval into sub-intervals, and each output class is associated to a MLNN at the next level. Then the number of output classes is gradually increasing from the first level to the last level, so TDNN can significantly improve the estimation accuracy by augmenting the depth of the tree instead of enlarging the scale of single network. Simulation results show that the proposed TDNN has much better performance than conventional DNN and root-MUSIC at low SNR, and can achieve CRLB.
- 2) To address the multi-emitter DOA measurement, TDNN is also extended to multi-emitter scenarios. Combining Q parallel TDNNs forms the Q -TDNN method, which can estimate Q different DOAs with same input. The

Y. Li, Jun Zou and Y. Song are with the School of Electronic and Optical Engineering, Nanjing University of Science and Technology, Nanjing 210094, China. (e-mail: liyifan97@foxmail.com).

F. Shu and Wei Gao are with the School of Information and Communication Engineering, Hainan University, Haikou 570228, China. (e-mail: shufeng0101@163.com).

J. Wang is with the School of Engineering, University of Kent, Canterbury CT2 7NT, U.K. (e-mail: j.z.wang@kent.ac.uk).

simulation results show that the proposed Q -TDNN has made a substantial performance enhancement over conventional methods with much lower computation complexity, and this gain grows as the number of emitters increases.

II. SYSTEM MODEL

Consider Q far-field narrow-band signals impinge onto an M -element uniform linear array (ULA). The q -th signal is expressed as $s_q(t)e^{j2\pi f_c t}$, where $s_q(t)$ is the baseband signal and f_c is the carrier frequency. Then the output signal at receive array is given by

$$\mathbf{y}(t) = \sum_{q=1}^Q \mathbf{a}(\theta_q) s_q(t) + \mathbf{v}(t) = \mathbf{A}(\boldsymbol{\theta}) \mathbf{s}(t) + \mathbf{v}(t), \quad (1)$$

where $\mathbf{a}(\theta_q) = [1, e^{j\frac{2\pi}{\lambda} d_0 \sin \theta_q}, \dots, e^{j\frac{2\pi}{\lambda} (M-1)d_0 \sin \theta_q}]^T$ is the array manifold vector, $\mathbf{A}(\boldsymbol{\theta}) = [\mathbf{a}(\theta_1), \mathbf{a}(\theta_2), \dots, \mathbf{a}(\theta_Q)]^T$, $\boldsymbol{\theta} = [\theta_1, \theta_2, \dots, \theta_Q]^T$ denotes the DOAs to be estimated and $\theta_1 < \theta_2 < \dots < \theta_Q$. $\mathbf{v}(t) \sim \mathcal{CN}(\mathbf{0}, \sigma_v^2 \mathbf{I}_M)$ represents the additive white Gaussian noise (AWGN) vector.

Following the signal model (1), the received signal's covariance matrix can be expressed as

$$\mathbf{R} = \mathbf{A} \mathbf{R}_s \mathbf{A}^H + \sigma_v^2 \mathbf{I}_M = \sum_{q=1}^Q \sigma_{s_q}^2 \mathbf{a}(\theta_q) \mathbf{a}^H(\theta_q) + \sigma_v^2 \mathbf{I}_M, \quad (2)$$

where $\mathbf{A} = \mathbf{A}(\boldsymbol{\theta})$ and $\mathbf{R}_s = \text{diag}\{\sigma_{s_1}^2, \dots, \sigma_{s_Q}^2\}$ denotes the signal power. However, since $\mathbf{a}(\theta)$ is unknown, the signal covariance matrix cannot be obtained directly, the sample covariance matrix $\tilde{\mathbf{R}} = \frac{1}{T} \sum_{t=1}^T \mathbf{y}(t) \mathbf{y}^H(t)$ is considered as a substitution and if $T \rightarrow \infty$, we have the sample covariance $\tilde{\mathbf{R}}$ is equal to the statistical \mathbf{R} in terms of the weak law of large number.

III. TREE-BASED DNN MODEL FOR HIGH-RESOLUTION DOA ESTIMATION

In this section, a novel tree model-based DNN (TDNN) model is proposed for high-resolution DOA estimation and its detailed training procedure is described as well.

A. Proposed Method

The proposed TDNN classifier is composed of H levels, and each level contains G_h fully-connected MLNNs, where $1 \leq h \leq H$. We let all the G_h networks in the same level of TDNN have identical structures, and their output layers all have L_h neurons. Then the sum output size of level h is $G_h L_h$, which is equal to the number of networks contained in level $(h+1)$, so G_{h+1} can be given by

$$G_{h+1} = G_h L_h = L_1 L_2 \cdots L_{h-1} L_h, \quad (3)$$

for $1 \leq h \leq H-1$ and $G_1 = 1$. As shown in Fig.1, the feature vector \mathbf{r} is firstly input to \mathcal{D}_1 , and the output layer of \mathcal{D}_1 has L_1 neurons. Then in order to join with the output size of level 1, level 2 contains L_1 networks, i.e., $G_2 = L_1$. So if a signal is divided into the class l_1 by \mathcal{D}_1 , where $1 \leq l_1 \leq L_1$, its corresponding feature vector \mathbf{r} will be then input to the l_1 -th network of level 2 ($\mathcal{D}_2^{l_1}$). After that, $\mathcal{D}_2^{l_1}$ has L_2 neurons

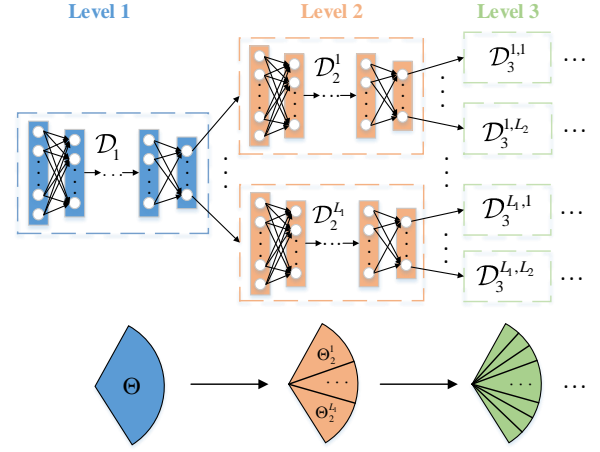


Fig. 1: Architecture of the proposed TDNN and the process of angular interval divided into sub-intervals by TDNN.

in its output layer, and there are also L_2 networks in level 3 connecting to it. Similarly, if the signal is labelled as class l_2 by $\mathcal{D}_2^{l_1}$, $1 \leq l_2 \leq L_2$, \mathbf{r} will be input to $\mathcal{D}_3^{l_1, l_2}$. Therefore, when TDNN is used to perform DOA estimation, only one network in each level will be activated. Thus the input feature vector is sequentially input to H networks, and by combining the classification results of these networks, we can obtain a H -dimensional numerical label vector $\boldsymbol{\ell} = [\ell_1, \ell_2, \dots, \ell_H]^T$, for $1 \leq \ell_h \leq L_h$ and $1 \leq h \leq H$. According to $\boldsymbol{\ell}$, the decision procedure that \mathbf{r} experienced in TDNN can be summarized as

$$\mathbf{r} \rightarrow \mathcal{D}_1 \xrightarrow{l_1} \mathcal{D}_2^{l_1} \xrightarrow{l_2} \dots \xrightarrow{l_{H-1}} \mathcal{D}_H^{l_1, l_2, \dots, l_{H-1}} \xrightarrow{l_H} \boldsymbol{\ell}, \quad (4)$$

where the lower right symbol of \mathcal{D} denotes the level number, and the upper right symbols represent the accumulative labels of the previous levels.

Since TDNN is designed for solving DOA estimation problems, we firstly consider the single emitter case, i.e., $Q = 1$, and assume the DOA θ must fall in an angular interval $\Theta = [\theta_{\min}, \theta_{\max})$, i.e. $\theta \in \Theta$, and it is divided into L_1 uniform sub-intervals by \mathcal{D}_1 like $\Theta = \bigcup_{l_1=1}^{L_1} \Theta_1^{l_1}$, where $\Theta_1^{l_1} = [\theta_{1,\min}^{l_1}, \theta_{1,\max}^{l_1})$. Then $\Theta_1^{l_1}$ can be further divided into smaller sub-intervals as $\Theta_1^{l_1} = \bigcup_{l_2=1}^{L_2} \Theta_2^{l_1, l_2}$, and $\Theta = \bigcup_{l_1=1}^{L_1} \bigcup_{l_2=1}^{L_2} \Theta_2^{l_1, l_2}$, where $\Theta_2^{l_1, l_2} = [\theta_{2,\min}^{l_1, l_2}, \theta_{2,\max}^{l_1, l_2})$. Therefore, level h of TDNN can divide Θ into $L_1 L_2 \cdots L_h$ uniform spatial subintervals, which is denoted by

$$\Theta = \bigcup_{l_1=1}^{L_1} \bigcup_{l_2=1}^{L_2} \dots \bigcup_{l_h=1}^{L_h} \Theta_h^{l_1, l_2, \dots, l_h} \quad (5)$$

where $\Theta_h^{l_1, l_2, \dots, l_h} = [\theta_{h,\min}^{l_1, l_2, \dots, l_h}, \theta_{h,\max}^{l_1, l_2, \dots, l_h})$. And we define the spatial resolution of level h as

$$\Delta \theta_h = \theta_{h,\max}^{l_1, l_2, \dots, l_h} - \theta_{h,\min}^{l_1, l_2, \dots, l_h} = \frac{\theta_{\max} - \theta_{\min}}{G_h L_h}, \quad (6)$$

where $\Delta \theta_1 > \Delta \theta_2 > \dots > \Delta \theta_H$. Therefore, the size of subintervals divided by the last level, i.e., $\Delta \theta_H = \theta_{H,\max}^{l_1, l_2, \dots, l_H} - \theta_{H,\min}^{l_1, l_2, \dots, l_H}$, represents the spatial resolution can be achieved by TDNN, which is expressed by

$$\Delta \theta = \Delta \theta_H = \frac{\theta_{\max} - \theta_{\min}}{G_H L_H} = \frac{\theta_{\max} - \theta_{\min}}{L_1 L_2 \cdots L_{H-1} L_H}, \quad (7)$$

where we can get $G_H = L_1 L_2 \cdots L_{H-1}$ based on (3). And the final estimated DOA $\hat{\theta}$ is related to the classification labels of all the levels, which is given by

$$\hat{\theta} = \theta_{min} + \ell^T \Delta \theta = \theta_{min} + \sum_{h=1}^H l_h \Delta \theta_h, \quad (8)$$

where $\Delta \theta = [\Delta \theta_1, \Delta \theta_2, \cdots, \Delta \theta_H]^T$. (7) and (8) show the DOA estimation accuracy of the proposed TDNN classifier depends on the values of H and L_h .

B. Training Procedure

All the MLNNs in the proposed TDNN classifier are composed of three parts, one input layer, one output layer and some hidden layers. Since the networks in the same level has the same number of input and output neurons, in order to reduce the training burden, we let the networks in the same level have the identical network structure, which means they have the same number of hidden layers and the same number of neurons. \mathcal{D}_h represents an arbitrary network in the level h of TDNN, supposing it has K layers including one input layer, one output layer and $K-2$ hidden layers, then the computation steps of the k -th layer in \mathcal{D}_h are given by

$$\mathbf{q}_h^k = \mathbf{W}_h^{k,k-1} \mathbf{g}_h^{k-1} + \mathbf{b}_h^k, \quad \mathbf{g}_h^k = A[\mathbf{q}_h^k], \quad (9)$$

where $1 \leq h \leq H$, $1 \leq k \leq K$. \mathbf{g}_h^k denotes the output vector in the k -th layer of \mathcal{D}_h , where $\mathbf{g}_h^0 = \mathbf{r}$ and \mathbf{g}_h^K is the output of \mathcal{D}_h . $\mathbf{W}_h^{k,k-1}$ represents the fully-connected weight matrix between the $(k-1)$ -th layer and n -th layer, and \mathbf{b}_h^k is the bias vector. $A[\cdot]$ denotes the activation function, it is set as ReLU function for hidden layers, while Softmax function for output layer.

In order to reduce the instability caused by the uncertain signal waveforms, we choose the signal sample covariance matrix \mathbf{R} as the input feature for the proposed TDNN classifier. In addition, due to the unknown noise variance and the lower left elements of \mathbf{R} are conjugate replicas of the upper right ones, then delete the redundant elements in \mathbf{R} and the final input vector is reformulated by the off-diagonal upper right elements of \mathbf{R} , given by

$$\mathbf{r} = [\text{Re}(\bar{\mathbf{r}}^T), \text{Im}(\bar{\mathbf{r}}^T)]^T \in \mathbb{R}^{M(M-1) \times 1}, \quad (10)$$

where $\bar{\mathbf{r}} = [R_{1,2}, \cdots, R_{1,M}, R_{2,3}, \cdots, R_{2,M}, \cdots, R_{M-1,M}]^T \in \mathbb{C}^{M(M-1)/2 \times 1}$ and $R_{i,j}$ denotes the (i,j) -th element of \mathbf{R} . In the prediction period, since the covariance matrix is unavailable, then the testset consists of the off-diagonal upper right elements of the sample covariance matrix $\hat{\mathbf{R}}$.

Since MLNNs in level h have same structures, let \mathbf{z}^h represent the one-hot form label vector for training \mathcal{D}_h , which is an $L_h \times 1$ binary vector with $\|\mathbf{z}^h\| = 1$ and its relationship with ℓ can be expressed as

$$\mathbf{z}^h(\ell(h)) = \mathbf{z}^h(l_h) = 1. \quad (11)$$

Therefore, by combining the training data and training label, the complete training set for the i -th MLNN is given as $\mathbb{T} = \{(\mathbf{r}, \mathbf{z}^h)\}$. Then we define $\hat{\mathbf{z}}^h$ as the output prediction vector of \mathcal{D}_h for \mathbf{r} , which is in the form of probability distribution.

So we choose binary cross entropy (BCE) as the loss function and it is given by

$$\text{loss} = -\frac{1}{L_h} \sum_{l_h=1}^{L_h} \left[\mathbf{z}^h(l_h) \log(\hat{\mathbf{z}}^h(l_h)) + (1 - \mathbf{z}^h(l_h)) \log(1 - \hat{\mathbf{z}}^h(l_h)) \right]. \quad (12)$$

Then the optimal weights and biases of \mathcal{D}_h can be obtained by minimizing this loss function.

C. Complexity Analysis

In the prediction stage, only one MLNN in each level of TDNN is activated for per DOA estimation, then the complexity of TDNN comes from two parts, i.e., model complexity and computation complexity. Firstly, we define the model complexity as the number of output classes required for achieving a specific resolution $\Delta \theta$, so the model complexity of conventional DNN is $\mathcal{M}(\text{DNN}) = O(N)$, where $N = (\theta_{max} - \theta_{min})/\Delta \theta$. Then the model complexity of TDNN is given by

$$\mathcal{M}(\text{TDNN}) = O\left(\sum_{h=1}^H L_h\right), \quad (13)$$

from (7) we know $N = L_1 L_2 \cdots L_H$, so it is obvious that $\mathcal{M}(\text{TDNN}) \ll \mathcal{M}(\text{DNN})$.

As discussed in [5], the computation complexity of a network is proportional to the number of layers and the number of neurons in each layer. So as the summation of all the activated MLNNs, the computation complexity of TDNN is

$$\mathcal{C}(\text{TDNN}) = O\left(\sum_{h=1}^H \sum_{k=1}^{K-1} W_h^k W_h^{k+1}\right), \quad (14)$$

where W_h^k denotes the number of neurons contained in the K -th layer of \mathcal{D}_h . And the comparison with the computation complexity of conventional DNN models will be displayed in simulation section.

IV. EXTENSIVE TDNN-BASED METHOD FOR MULTI-EMITTER SCENARIOS

As the number of signal sources increases, the corresponding DOA estimation problem is converted into a multi-label learning problem. For conventional DNN-based DOA estimation algorithms, each unit in the output layer corresponds to an independent angle, so when the combined signals from Q different sources are input to the DNN, the training label vector will be a binary vector \mathbf{z}_{DNN} which contains Q '1' elements, i.e., $\|\mathbf{z}_{\text{DNN}}\|_1 = Q$. However, for our proposed TDNN, since the output neurons of each level correspond to different angular regions, it is possible that several DOAs in the same region under the multi-emitter case, then there will appear that different signals marked by same label and thus the binary vector cannot express it. Therefore, we give an $L_h \times Q$ binary label matrix for classifying the Q -emitters signals input to \mathcal{D}_h

$$\mathbf{Z}^h = [\mathbf{z}_1^h, \mathbf{z}_2^h, \cdots, \mathbf{z}_Q^h], \quad (15)$$

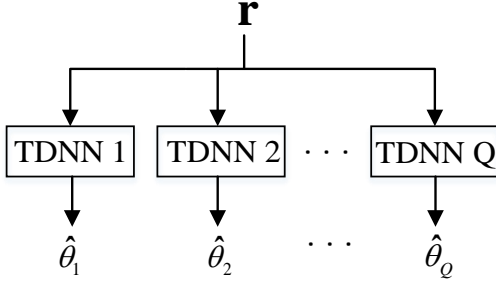


Fig. 2: Proposed Q -TDNN for multi-emitter DOA estimation.

where \mathbf{z}_q^h denotes the one-hot form label vector of the q -th signal and $\|\mathbf{z}_q^h\|_1 = 1$.

Since the feature vector \mathbf{r} is only constructed by the upper right elements of \mathbf{R} and has no connection with noise, then by observing (2) that \mathbf{r} can be separated into Q components under Q -sources cases as

$$\mathbf{r} = \mathbf{r}_1 + \mathbf{r}_2 + \cdots + \mathbf{r}_Q, \quad (16)$$

where \mathbf{r}_q is the feature component of θ_q and its elements are from the upper right part of $\sigma_{s_q}^2 \mathbf{a}(\theta_q) \mathbf{a}^H(\theta_q)$. Therefore, by drawing on the idea of binary relevance, we consider transforming the Q -emitters DOA estimation problem into Q single-source problems. And when solving the q -th problem, we can regard \mathbf{r}_q as the principal component and \mathbf{r} is classified as θ_q . Then the Q -TDNN algorithm is proposed based on this principle.

As shown in Fig.2, Q -TDNN is composed of Q TDNNs with same structures, and TDNN q is used to solve the q -th problem. Firstly, \mathbf{r} is separately input to these Q TDNNs, $\ell_q = [l_{q,1}, l_{q,2}, \cdots, l_{q,H}]^T$ denotes classification result of TDNN q , then we can obtain the estimation result of θ_q as

$$\hat{\theta}_q = \theta_{min} + \ell_q^T \Delta \theta = \theta_{min} + \sum_{h=1}^H l_{q,h} \Delta \theta_h, \quad (17)$$

then by combining all the Q results, the complete DOA estimation result of Q -TDNN is given as $\hat{\theta}_{Q\text{-TDNN}} = [\hat{\theta}_1, \hat{\theta}_2, \cdots, \hat{\theta}_Q]$.

Since the Q -TDNN contains Q TDNNs, and they have the same architectures, then the computation complexity of Q -TDNN is given by

$$\mathcal{C}(Q\text{-TDNN}) = Q \cdot \mathcal{C}(\text{TDNN}). \quad (18)$$

V. SIMULATION RESULTS

In this section, the DOA estimation performance of the proposed methods is verified by performing a series of numerical simulations. The receive array is equipped with a 16-elements ULA, the interelement spacing of the ULA is half-wavelength, and the DOAs of all the signals are fall in the angular region $\Theta = [-60^\circ, 60^\circ]$. These simulations are implemented on Tensorflow. The proposed TDNN method is mainly compared to DNN and root-MUSIC, where the fully-connected DNN considered in this work is a widely used DL model in the DOA estimation [10] [11] and root-MUSIC [12] is a classical subspace-based off-grid DOA estimation algorithm.

TABLE I: Model parameters.

	H	G_h	Network structures		
			input layer	hidden layers	output layer (L_h)
2-Level TDNN	2	1	240	32, 16, 16	12
		12	240	32, 16, 16	10
3-Level TDNN	3	1	240	32, 16, 16	6
		6	240	32, 16, 16	5
		30	240	32, 16, 16	4

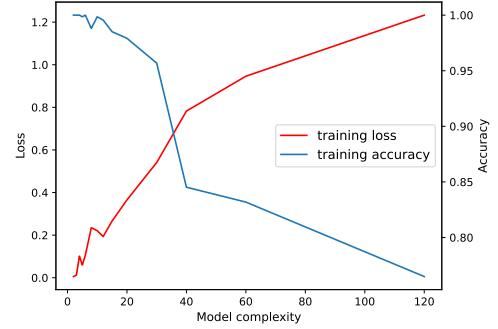


Fig. 3: Relationship between training performance and model complexity of DNN

Table I lists the model parameters of the proposed TDNN, where H denotes the depth of TDNN and G_h represents the number of MLNNs contained in each level. The network structures of 2-level TDNN and 3-level TDNN are also shown in this Table. In addition, we select Adam as the optimizer, with batch size, epochs and learning rate being 1000, 100 and 0.01 respectively.

Fig.3 plots the training performance versus the model complexity of DNNs. From this figure, it is seen that the model accuracy of DNNs becomes worse with the increasing of output classes. This means small-scale networks can have better model accuracy than large-scale networks. The specific impact on DOA estimation performance will be analyzed in the following by combining Fig.4.

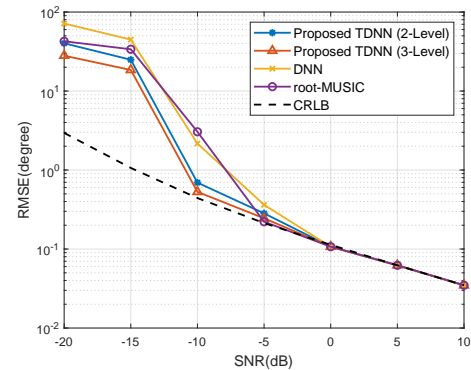


Fig. 4: RMSE versus SNR.

Fig.4 demonstrates the DOA RMSE versus SNR of the proposed TDNN with DNN, root-MUSIC and CRLB. The specific parameters involved in this simulation are as follows:

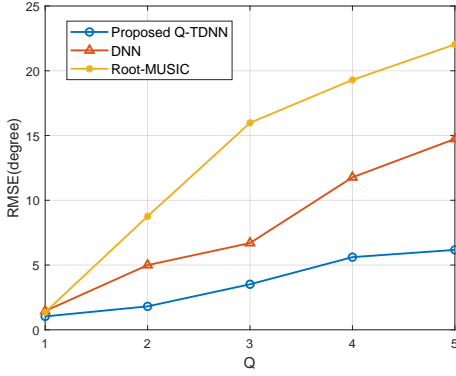


Fig. 5: RMSE versus the number of emitters.

$N = 50$, $Q = 1$ and $\theta = 27^\circ$. From this figure, it can be seen that TDNN attains obvious performance gains over conventional DNN and root-MUSIC at $\text{SNR} < -5\text{dB}$. TDNN can also nearly achieve CRLB at $\text{SNR} = -5\text{dB}$, while root-MUSIC can only achieve it at $\text{SNR} = -10\text{dB}$. Additionally, the comparison between TDNNs with different structures is noteworthy. The performance of 3-level TDNN is better than 2-level TDNN, and from Table I we can find the model complexity of 3-level TDNN is also lower than 2-level TDNN. Therefore, by combining the conclusion of Fig.3, we can conclude lower model complexity makes higher DOA estimation accuracy, and it is a key index must be considered when a TDNN model is constructed.

Fig.5 depicts the DOA estimation RMSE versus of Q -TDNN, DNN and root-MUSIC under the multi-emitter scenarios and $\text{SNR} = -8\text{dB}$. It can be seen from this figure the RMSE of these three methods are very close when $Q = 1$, but as the number of emitters increases, the performance gap between the other two methods and TDNN is increasing, when $Q = 5$, Q -TDNN has about 16° performance advantage over root-MUSIC and 8.5° over DNN. Therefore, the proposed Q -TDNN is confirmed to be a much more accurate method for the multi-emitter cases.

Finally, Fig.6 shows the computation complexity of TDNNs and DNN. TDNN is equivalent to Q -TDNN as $Q \geq 2$. Since the structure of conventional DNN keeps invariant with the increases of Q , its computation complexity is also fixed. As TDNN only activates one network in each level for per DOA estimation, the computation complexity of TDNN is significantly lower than that of DNN with any structures. Then combining Fig.5 and Fig.6, it can be concluded that TDNN is a much better model than conventional DNN because it can achieve significantly higher accuracy with much lower computation complexity.

VI. CONCLUSIONS

In this work, a novel multi-level tree-based DNN model for high-resolution DOA estimation was proposed. Each level of TDNN adopts small-scale MLNNs as nodes to partition the target angular interval into multiple sub-intervals and each output class is associated to a MLNN at the next level. As the number of MLNNs increases from the first level to the last level, and so as the sum output classes. Therefore, TDNN

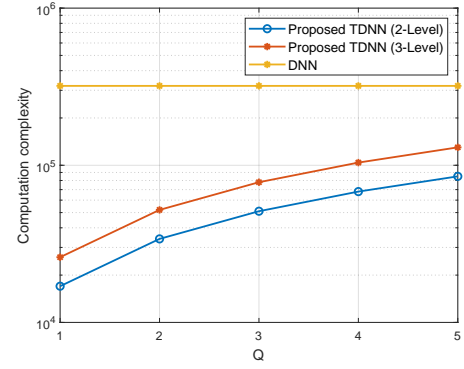


Fig. 6: Computation complexity versus the number of emitters.

can improve the DOA estimation accuracy by adding the number of levels without increasing the model complexity of each MLNN. The proposed TDNN performs much better than conventional methods like Root-MUSIC, DNN when SNR is in the extremely low region ($< -5\text{dB}$). Additionally, Q -TDNN method is also designed for multi-emitter scenarios on basis of TDNN. The performance enhancement of Q -TDNN over DNN and root-MUSIC also increases as the number of emitters increases.

REFERENCES

- [1] R. W. Heath, N. Gonzalez-Prelcic, S. Rangan, W. Roh, and A. M. Sayeed, "An overview of signal processing techniques for millimeter wave MIMO systems," *IEEE J. Sel. Topics Signal Process.*, vol. 10, no. 3, pp. 436–453, 2016.
- [2] L. Cheng, Y.-C. Wu, J. Zhang, and L. Liu, "Subspace identification for DOA estimation in massive/full-dimension MIMO systems: Bad data mitigation and automatic source enumeration," *IEEE Trans. Signal Process.*, vol. 63, no. 22, pp. 5897–5909, 2015.
- [3] F. Shu, Y. Qin, T. Liu, L. Gui, Y. Zhang, J. Li, and Z. Han, "Low-complexity and high-resolution DOA estimation for hybrid analog and digital massive MIMO receive array," *IEEE Trans. Commun.*, vol. 66, no. 6, pp. 2487–2501, 2018.
- [4] H. Huang, J. Yang, H. Huang, Y. Song, and G. Gui, "Deep learning for super-resolution channel estimation and DOA estimation based massive MIMO system," *IEEE Trans. Veh. Technol.*, vol. 67, no. 9, pp. 8549–8560, 2018.
- [5] D. Hu, Y. Zhang, L. He, and J. Wu, "Low-complexity deep-learning-based DOA estimation for hybrid massive MIMO systems with uniform circular arrays," *IEEE Wireless Commun. Lett.*, vol. 9, no. 1, pp. 83–86, 2019.
- [6] G. K. Papageorgiou, M. Sellathurai, and Y. C. Eldar, "Deep networks for direction-of-arrival estimation in low SNR," *IEEE Trans. Signal Process.*, vol. 69, pp. 3714–3729, 2021.
- [7] L. Wu, Z.-M. Liu, and Z.-T. Huang, "Deep convolution network for direction of arrival estimation with sparse prior," *IEEE Signal Process. Lett.*, vol. 26, no. 11, pp. 1688–1692, 2019.
- [8] X. Wu, X. Yang, X. Jia, and F. Tian, "A gridless DOA estimation method based on convolutional neural network with Toeplitz prior," *IEEE Signal Process. Lett.*, vol. 29, pp. 1247–1251, 2022.
- [9] M.-L. Zhang and Z.-H. Zhou, "A review on multi-label learning algorithms," *IEEE Trans. Knowl. Data Eng.*, vol. 26, no. 8, pp. 1819–1837, 2013.
- [10] S. Xu, A. Brighente, B. Chen, M. Conti, X. Cheng, and D. Zhu, "Deep neural networks for direction of arrival estimation of multiple targets with sparse prior for line-of-sight scenarios," *IEEE Trans. Veh. Technol.*, vol. 72, no. 4, pp. 4683–4696, 2022.
- [11] A. M. Ahmed, U. S. K. M. Thanthirige, A. El Gamal, and A. Sezgin, "Deep learning for DOA estimation in MIMO radar systems via emulation of large antenna arrays," *IEEE Commun. Lett.*, vol. 25, no. 5, pp. 1559–1563, 2021.
- [12] A. Barabell, "Improving the resolution performance of eigenstructure-based direction-finding algorithms," in *ICASSP'83. IEEE International Conference on Acoustics, Speech, and Signal Processing*, vol. 8. IEEE, 1983, pp. 336–339.